ISSN NO. 2320-5407

Journal homepage: http://www.journalijar.com

INTERNATIONAL JOURNAL OF ADVANCED RESEARCH

RESEARCH ARTICLE

Study on inclusion complex behaviours of L-Tyrosine and β-Cyclodextrin by Cyclic Voltammetric technique using Glassy carbon electrode

S. Mohandoss and T. Stalin*

Department of Industrial Chemistry, School of Chemical Sciences, Alagappa University, Karaikudi- 630 003, Tamilnadu, India.

Manuscript Info

Manuscript History:

Received: 12 June 2013
Final Accepted: 19 June 2013
Published Online: July 2013

Key words:
Inclusion complex, β-Cyclodextrin, L-Tyrosine, Surfactants, Glassy carbon electrode, Cyclic voltammetry

Abstract

The inclusion complex between L-Tyrosine (L-TY) and β-Cyclodextrin (β-CD) is investigated by cyclic voltammetric technique using glassy carbon electrode (GCE). Peak currents (I_{pa} & I_{pc}) drastically changes with increasing β-CD concentration and the peak potentials (E_{pa} & E_{pc}) shifted towards the positive direction for this inclusion complex. The formation of 1:1 inclusion complex has been confirmed by Benesi-Hildebrand plot and the schematic diagram was proposed and explains for this inclusion complex process. The binding constant of inclusion complex at 303 K is calculated and a thermodynamic parameter (ΔG) also calculated. The effect of surfactant studies carried out using Sodium dodecyl sulphate (SDS), cetyltrimethylammonium bromide (CTAB) and octylphenolpoly(ethyleneglycolether)$_n$ n=10, Triton X-100 (TRX-100). Among these surfactants, CTAB only shows excellent enhancement in both oxidation (+4.5753 μA, +3.4359 μA) and reduction (-1.4126 μA) peak currents.

Introduction

Electrochemistry of cyclodextrins (CDs) and cyclodextrin inclusion complexes with different organic compounds was studied by several authors (Ming et al., 2006, Longzhen 2008 and Gharibi 2000). One of the most important characteristics of CDs is the formation of inclusion complexes with various organic and inorganic guest molecules (Szejtli et al., 1982). Upon inclusion complexation, the characteristic properties of the guest molecule inside the CDs cavities, such as electrochemical properties will be changed significantly.

Cyclodextrins (CDs) are cyclic oligosaccharides consisting of 6, 7, and 8 units of 1,4-linked glucose units, and are named alpha (α), beta (β) and gamma (γ)- Cyclodextrins, respectively (Scheme 1a). These macromolecules, which can be spatially represented as a torus with wide and narrow openings corresponding to secondary and primary hydroxyl groups respectively, can encapsulate a large variety of compounds due to the hydrophobic character of their internal cavity (Alan et al., 2003). Although the depth of the cavities for the three CDs is the same (~0.78 nm), their cavity diameters are ~0.57, 0.78 and 0.95 nm respectively (Scheme 1b). Due to the unique chemical structure of CD molecules, the inner side of the cavity is hydrophobic and the outer side is hydrophilic. The hydrophobic nature of the CD cavities facilitates the ability of CDs to act as host for both non-polar and polar guests, which include small molecules as well as polymers (Xintao et al., 2001). The inclusion complexes depend on the size and the polarity of the guest molecules, the nature of the pH solutions. However, the proposed for the driving forces for the CDs inclusion complexation, including vander waals interactions and hydrophobic interactions between the hydrophobic moiety of the guest molecules and the CD cavity, hydrogen bonding between the polar functional groups of the guest molecules and the hydroxyl groups of CDs, release of high-energy water in the cavity in the complex formation, and release of strain energy in the ring frame system of the CD. Among those forces, hydrophobic interactions are frequently considered as the main

driving force for the complexation in aqueous media between host and guest molecules.

Electro analytical methods measuring the current response to the potential applied allow monitoring changes in the redox state of the electro active sites in CD-based systems. Cyclic voltammetries are the most frequently employed electrochemical techniques for electro active CDs systems. They provide useful information on the reduced nature and oxidized forms of the compounds, and on the mechanistic aspects of the electrode processes. They also allow monitoring even very subtle changes of the molecular environment of the redox centers by following their redox potentials. Among the various approaches for the determination of binding constants, electrochemical methods are very useful, especially when the guest molecule is electroactive molecules. In the case of a reversible electrochemical reaction process, in which an inclusion complex is formed between an electroactive guest and a host molecules (Srinivasan et al., 2012). The formation of inclusion complexes is the point of interest in most electrochemical investigations of CDs in solution. Binding constants in solution are usually determined from the plots of cyclic voltammetry peak potentials versus CDs concentration after assessing the guest/host ratio in the complex.

L-Tyrosine (L-TY) is one important amino acid to establish the molecules of proteins (Scheme 2). L-TY is the precursor of dopamine, thyroxin and neurotransmitters in mammalian central nervous systems (Qiao et al., 2005). L-TY is essential for human to establish and maintain nutritional balance (Carlsson et al., 1978). Many methods have been applied for the measurement of L-Tyrosine, including fluorometric methods (Fang et al., 2006), chemiluminescence (Sanfeliu et al., 2003), spectrometric analysis (Chung et al., 2006), high-performance liquid chromatography (Sabine et al., 1997) capillary electrophoresis (Ying et al., 2006) infrared chemical sensor (Huei et al., 2008) electrochemical sensor (Carmen et al., 2010), and thin films (Kenneth et al., 2009), and Protein tyrosine kinase activity (Kagan et al., 2009). Recently, electrochemical methods have been found in many applications in the determination of electroactive amino acids because of their inherent electroactivity of thiol or aromatic groups, including cysteine, tyrosine and tryptophan (MacDonald et al., 1996).

Surfactant is a linear molecule with a hydrophilic (attracted to water) head and a hydrophobic (repelled by water) end. The interaction between surfactant and proteins has been recognized for a long time. Amino acids are important biological-active substances and basic structural units of proteins. The study on the effect of amino acid on the properties of surfactant will provide the important information for interaction between surfactant and protein. The study on the property of the aqueous solution of amino acids is very limited and there appears to have been only several studies in the first half of the 20th century (Pappenheimer et al., 1936). The studies have intended to explore surface properties of zwitterionic solutes and showed general tendencies of the solutions. Due to its unique molecular structure, surfactant was extensively used in the fields of electrochemistry and electroanalytical chemistry for various purposes (Hu et al., 1991 and James 1991). For example, the addition of surface-active agents to electrolyte containing terazosin enhanced the voltammetric peak response at GCE (Nada et al., 2007). Surfactants containing hydrophobic and hydrophilic groups, can change the properties of the electrode/solution interface and subsequently influence the electrochemical processes of other substances (Hu et al., 1991). Adsorption of surfactants aggregates on the electron transfer, gently enhance the peak current, change the redox potential or charge transfer coefficients or diffusion coefficients, as well as alter the stability of electrogenerated intermedietes or electrochemical products. (Yi, H et al., 2001) Group has introduced surfactants to electroanalytical chemistry to improve the detection limits of some biomolecules. The results showed that the electrochemical responses of these compounds were greatly enhanced in the presence of trace surfactants.

The corresponding author has been largely involved in studying the electrochemical properties (Srinivasan et al., 2011 and Srinivasan 2011) of different organic compounds. In the present work, this stimulated us to preliminarily carry out to the study of the host-guest inclusion complex by electrochemical technique in different pH buffers. This might be able to explain the enhancement effects of three surfactants in electroanalytical method for L-TY. The L-TY based on the increase in the current signal of oxidation and reduction at bare GCE in the presence of three surfactants (Scheme 3) like sodium dodecyl sulphate (SDS), cetyltrimethyl ammonium bromide (CTAB) and octylphenolpoly(ethyleneglycolether)$_n$ n = 10, Triton X-100 (TRX-100) at glassy carbon electrode was explored by cyclic voltammetry.

Experimental

Reagents

β-Cyclodextrin received from Sigma-Aldrich Chemical India, Bangalore and L-Tyrosine (L-TY) (Sisco Research Laboratories) used as commercial. Sodium dodecyl sulphate (SDS),

Cetyltrimethyl ammonium bromide (CTAB) and Triton X-100 (TRX-100) were purchased from (Sd fine chemical company) and used without further purification. All other reagents were of analytical grade and all the solutions were prepared from tribly distilled water. Standard solution of L-Tyrosine ($2.7x10^{-3}$ mol dm^{-3}) was prepared by dissolving the requisite amount of L-Tyrosine in minimum quantity of 0.1 M H_2SO_4 and then diluted to the desired concentration with deionized water. All the stock solution prepared in pH~7 (0.1 M KH_2PO_4 + 0.1 M NaOH) phosphate buffer solution. β-Cyclodextrin; 0, 2, 4, 6, 8, 10, $12x10^{-3}$ mol dm^{-3} and SDS, CTAB, and TRX-100; 0, 1, 2, 3, 4, $5x10^{-4}$ mol dm^{-4}.

Apparatus

Electrochemical experiments were carried out using autolab electrochemical analyzer it used to apply potential on the working equipped with a three-electrode system using glassy carbon electrode (GCE) (diameter: 1 mm) is served as a working electrode. Reference electrode (Ag/AgCl) was saturated calomel electrode (SCE) and platinum wire as counter electrode. All experiments were carried out at 30 $\pm1^{o}$C. The working electrode was polished to a mirror with 0.05 µm alumina slurry, and rinsed with triply distilled water before each experiment. A digital pH/mV meter (ELICO LI 120) was used for pH measurements.

Result and discussion

Influence of pH

The effect of solution pH on the L-tyrosine current response in the range of pH 1 to 12 investigate any influence of the pH of the buffer solution on the electrochemical reaction carry out (Li et al., 2006), the effect of different electrolytes (pH~1 to pH~12) on the current response was investigated by cyclic voltammetry. Fig. 1 shows that the electrode process is pH dependent and it's suggesting that the electrochemical reaction mechanism of this oxidation behavior in aqueous media involves the same number of electrons and protons. Normally, the electrochemical analysis showed that the oxidation behavior proceeds at the aromatic nucleus, through an electron transfer process, though the formation of a monocation that undergoes further acid-base prototropic reaction. For pH values between 2 and 6, no significant variation in the peak current was observed. But pH values in pH~1 and pH~7, a broad and higher peak current was observed. Fig. 1 shows that the electrochemical signal of L-Tyrosine oxidation is pH dependent and reaches maximum values in the range of 6–7. In further studies, pH~7 was employed. Further, this buffer was chosen as the best supporting electrolyte and was used throughout the host-guest inclusion complex and electro-analytical studies. The effect of temperature (0-30^{o}C) on peak current and peak potential of L-TY was observed. The result shows that the peak current increases and the peak potential are almost unchanged with the increasing temperature. So the temperature 30 $\pm1^{o}$C was followed for all further works.

Electrochemical oxidation of L-Tyrosine (L-TY)

L-Tyrosine contains pH-sensitive groups, including NH_2, OH and COOH; therefore, pH may affect the composition and the electrochemical oxidation of L-TY. Cyclic voltammograms (CVs) of $2.7x10^{-3}$ M L-Tyrosine at different pH values were recorded at the GCE (Fig. 1). The possible mechanism of the electrochemical oxidation of L-TY in acid, neutral and base medium are given in Scheme 4. As a function of pH, at the very lower pH values, L-TY has a protonated $R\text{-}NH_3^+$. As pH increases, the OH group proton is lost at above pH~7, resulting in formation of the O^- anion. The O^- anion in the L-TY with the neighboring $R\text{-}NH_3^+$ groups on the same (or a neighboring monomer) to form zwitterions, known to possess low solubility. At a pH~7, the -COOH group is followed by the deprotonation at above pH~7. This result in a dianion at pH values above 7, leading to the highest hydrophilicity measured at pH~7 for the L-TY. Therefore, presence of –OH group is responsible for the proton transfer. Cyclic voltammograms for the electrochemical oxidation of $2.7x10^{-3}$ M L-Tyrosine with β-cyclodextrin and surfactants in phosphate buffer solution at pH~7, as shown in Fig. 5a and 9a (Scheme 5).

Cyclic voltammetric studies of inclusion complex

The spectroscopic study reported by corresponding author (Shanmugam et al., 2008) related to the L-TY and β-CD interaction, based on this report, the electrochemical studies have been carried out to investigate the enhancement effect of β-CD with L-TY on glassy carbon electrode (GCE) as working electrode. The influence of the β-CD on the cyclic voltammograms of L-TY can be shown in Fig.2 and 3.

Fig.1. The pH influence of L-Tyrosine (L-TY)

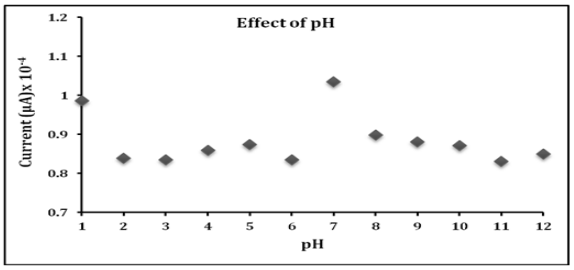

Fig.2. Cyclic voltammetric study for L-TY:β-CD in pH~1 buffer, scan rate 100 mVs^{-1}, L-TY. (Conc.2.7x10^{-3} M) solution in various concentration of β-CD. Inset figure; Benesi– Hildebrand plot of $1/I_G - I_{HG}$ vs. 1/[β-CD].

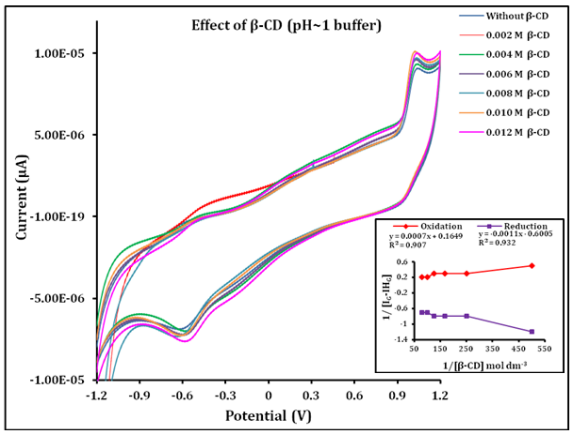

Fig.3. Cyclic voltammetric study for L-TY:β-CD in pH~7 buffer, scan rate 100 mVs^{-1}, L-TY. (Conc.2.7x10^{-3} M) solution in various concentration of β-CD. Inset figure; Benesi–Hildebrand plot of $1/I_G - I_{HG}$ vs. 1/[β-CD].

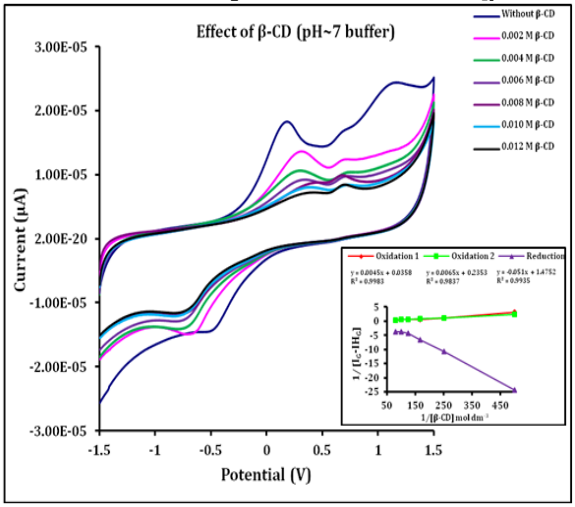

Fig.4. The peak current of L-TY changes at oxidation and reduction peak current with various.β-CD concentrations in (a) pH~1 and (b) pH~7 buffers respectively.

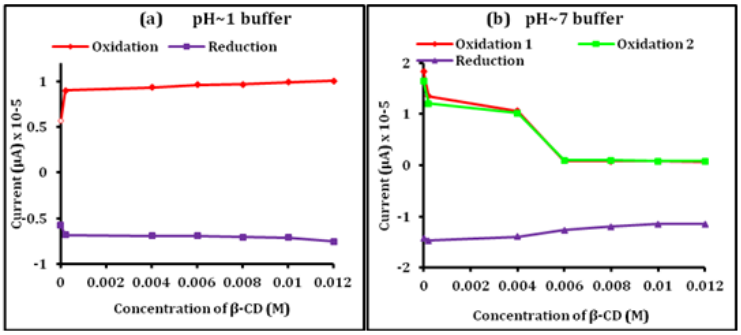

Fig. 5 (a) Cyclic voltammograms of 2.7x10^{-3} M L-Tyrosine at GCE in β-cyclodextrin (b) Graphical representation of current enhancement of 2.7x10^{-3} M L-Tyrosine at GCE in β-cyclodextrin

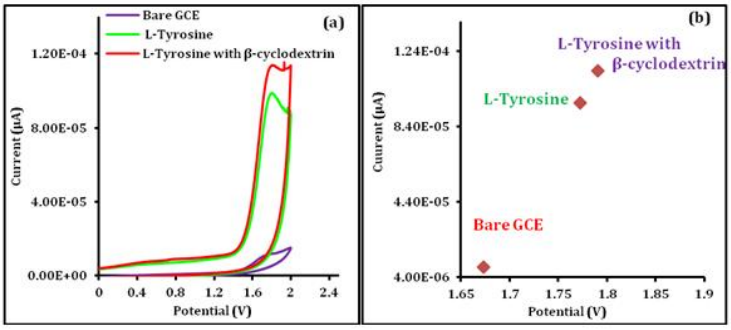

Fig.6. Cyclic voltammetric study for L-TY:SDS in pH 7 buffer, scan rate 100 mVs^{-1}, L-TY (Conc.2.7x10^{-3} M) solution in various concentration of SDS. Inset figure; Benesi–Hildebrand plot of $1/I - I_0$ vs. 1/[SDS].

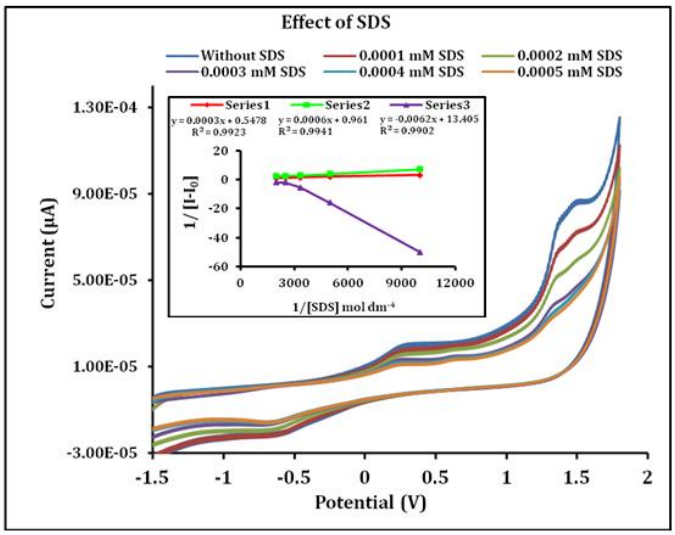

Fig.7. Cyclic voltammetric study for L-TY:CTAB in pH 7 buffer, scan rate 100 mVs^{-1}, L-TY (Conc.$2.7x10^{-3}$ M) solution in various concentration of CTAB.Inset figure; Benesi–Hildebrand plot of $1/I - I_0$ vs. 1/[CTAB].

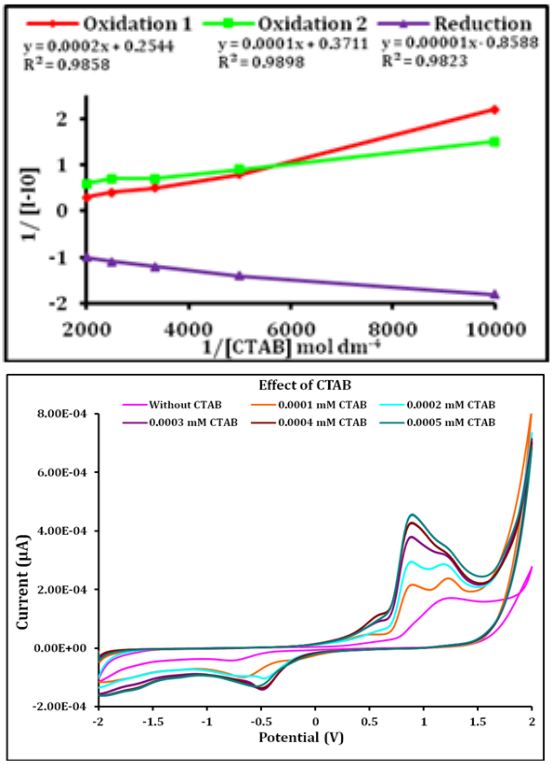

Fig.8. Cyclic voltammetric study for L-TY:TRX-100 in pH 7 buffer, scan rate 100 mVs^{-1}, L-TY (Conc.$2.7x10^{-3}$ M) solution in various concentration of TRX-100.Inset figure; Benesi–Hildebrand plot of $1/I - I_0$ vs. 1/[TRX-100].

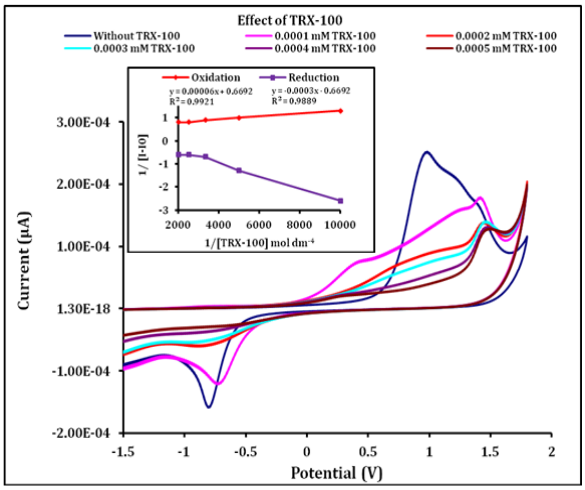

Fig. 9 (a) Cyclic voltammograms of $2.7x10^{-3}$ M L-Tyrosine at GCE in surfactants (b) Graphical representation of current enhancement of $2.7x10^{-3}$ M L-Tyrosine at GCE in β-cyclodextrin

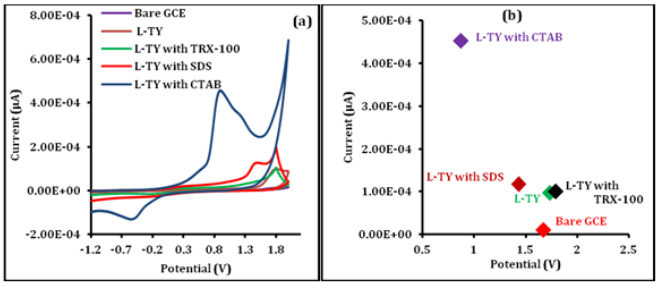

Fig.10. The peak current of L-TY changes at oxidation and reduction peak current with various (a) SDS, (b) CTAB and (c) TRX-100 concentrations in pH 7 buffer respectively.

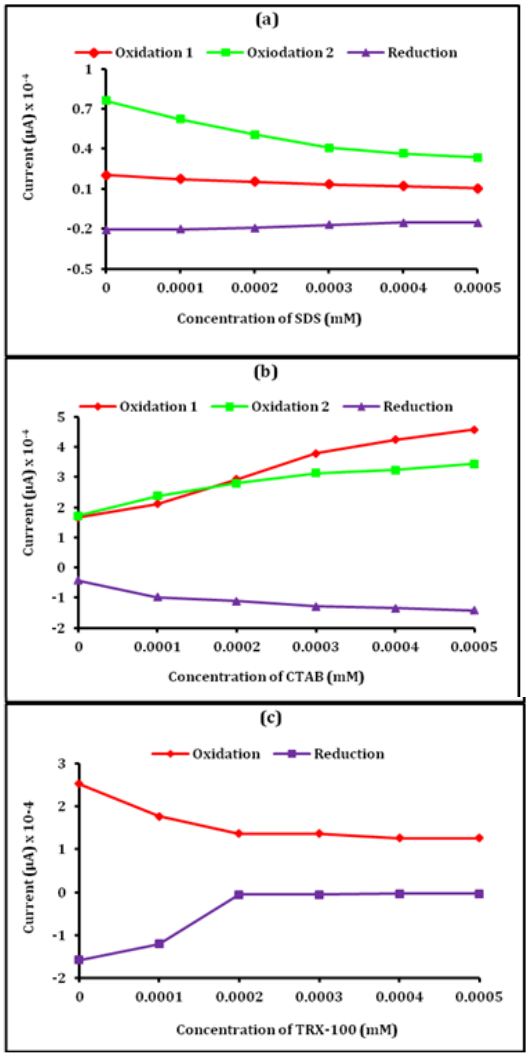

Fig.11. Graphical representation of peak current enhancement of 2.7x10^{-3} M L-Tyrosine/GCE at (a) oxidation (b) reduction peak current with various surfactants concentrations in pH~7 buffer respectively.

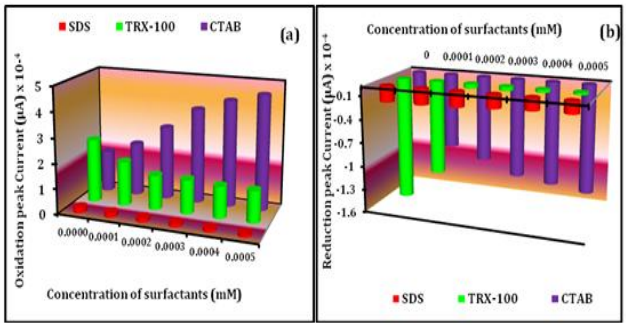

From Fig.2 (pH~1 buffer) and Fig.3 (pH~7 buffer) the anodic peak current (I_{pa}), decreased drastically with increasing the concentration of β-CD in pH~1 and pH~7 solution. The anodic peak potential (E_{pa}) shifted in positive direction when β-CD is increased in both cases. The results showed that inclusion complex between β-CD and L-TY was formed when β-CD was added into L-TY aqueous solution. The diffusion co-efficient of the inclusion complex from bulk layer to electrode surface was very slow than that of the L-TY molecule itself, which leaded the current decrease. On the other hand, because L-TY molecule entered into the hydrophobic cavity of β-CD, it was reasonable for that the electrochemical oxidation of the inclusion complex was more difficult than that of L-TY molecule itself, which would lead the anodic peak potential shift in positive direction, the anodic peak current (I_{pa}) decreased.

The oxidation potential of L-TY is +1.0356 V and +0.1771 V, +0.6582 V and the reduction potential is -0.5801 V and -0.4867 V, observed in pH~1 and pH~7 respectively. The difference between the oxidation and reduction potential is 807 mV and 332 mV, 572 mV for pH~1 and pH~7 respectively, so this reaction in both pH medium is quasi reversible. Increasing the β-CD concentration from 0 to 12x10^{-3} M the difference between the oxidation and reduction potential value also decreased to 785 mV in pH~1 and increased 578 mV, 755 mV in pH~7 solutions. Because, this molecule moves towards irreversible and L-TY entered into the hydrophobic cavity of β-CD, it was reasonable that the electrochemical oxidation of the inclusion complex was more difficult than that of L-TY molecule itself.

The oxidation potential of L-TY in pH~1 is higher (+1.0356 V) than pH~7 (+0.1771 V and +0.6582 V), this is due to the formation of monocation in pH~1, because of this monocation form, oxidation occurs at higher potential (+1.0356 V) and the peak current also increases (+0.8792 μA) due to the loss of electrons simultaneously protonation (H^+) to occurs in L-TY. It is found that the potentials (E_{pa}) shifted negatively with increasing pH, it indicating that protons takes part in the oxidation process of L-TY at the GCE surface. The anodic peak potential (E_{pa}) and cathodic peak potential (E_{pc}) is proportional to the pH solution in the range of pH~1 to pH~12. The linear-regression of L-TY is described as following with the correlation co-efficient (R^2) = 0.9070, 0.9320 in pH~1 and 0.9983, 0.9837 and 0.9935 obtained in pH~7 respectively. The relationships between the potentials and pH were linear, and the regression value gives as follows;

E_{pa} (V) = 0.1649 – 0.0007 pH; E_{pc} (V) = -0.6005-0.0011 pH …… (pH~1)

E_{pa} (V) = 0.0358 – 0.0045 pH; E_{pc} (V) = -1.4752-0.0510 pH …… (pH~7)

In pH~7 the lone pair of electron get oxidized at lower potential (+0.1771 V and +0.6582 V) and peak current also decreases (+1.8301 μA and +1.6412 μA).

$$\frac{1}{I_G - I_{HG}} = \frac{1}{\Delta I} + \frac{1}{K[\text{L-TY}]_0 \, \Delta I \, [\beta\text{-CD}]_0}$$

where I_G is the oxidation peak current of guest molecule of L-TY, and I_{HG} is the oxidation peak current of inclusion complex of L-TY: β-CD and I_G - I_{HG} difference between the oxidation peak current of L-TY and L-TY: β-CD inclusion complex, is the difference between the peak current co-efficient of L-TY and the inclusion complex, $[\text{L-TY}]_0$ and $[\beta\text{-CD}]_0$ are the initial concentration of L-TY and β-CD, respectively.

A plot of $1/I_G$-I_{HG} versus $1/[\beta\text{-CD}]$ gives a straight line for pH~1 and pH~7 buffer solutions as shown in Fig.2 and 3 (inset figures). Good linear correlations were obtained, confirming that the formation of a 1:1 inclusion complex for pH~1 and pH~7 solutions. The binding constant K and stoichiometric ratios of the inclusion complex of L-TY can be determined according to the Benesi-Hildebrand relation assuming the formation of a 1:1 host–guest inclusion complex between β-CD and L-TY (Scheme 6). From the intercept and slope values of this plot binding constant 'K' values was evaluated, the binding constant for L-TY: β-CD was 324 M^{-1}and 514 M^{-1} in pH~1 and 138 M^{-1} and 142 M^{-1}, 69 M^{-1} in pH~7 solution. When the β-CD concentrations higher than 12 x10^{-3} mol dm^{-3}, the oxidation peak current remain unchanged by further

addition of β-CD in pH~1 and pH~7 (Fig.4a and 4b) solutions. This behavior has been attributed to the enhanced dissolution of the L-TY molecule through the hydrophobic interaction between L-TY and β-CD. These results indicate that L-TY molecule is entrapped in the nano hydrophobic β-CD cavity to form inclusion complex and it proved by electrochemically. The neutral species of L-TY was predominant at pH~6 to 7. While in acidic and basic media, the neutral form gradually decreased and the deprotonated and protonated form of L-TY was predominant. We noted that the β-CD can readily include the neutral form, which was more hydrophobic than the ionized form (Geoffrey et al., 1987). Therefore, phosphate buffer solution at pH~7 was chosen to obtain the maximum oxidation currents of L-TY.

Scheme 1. The structure of α, β and γ-Cyclodextrins.

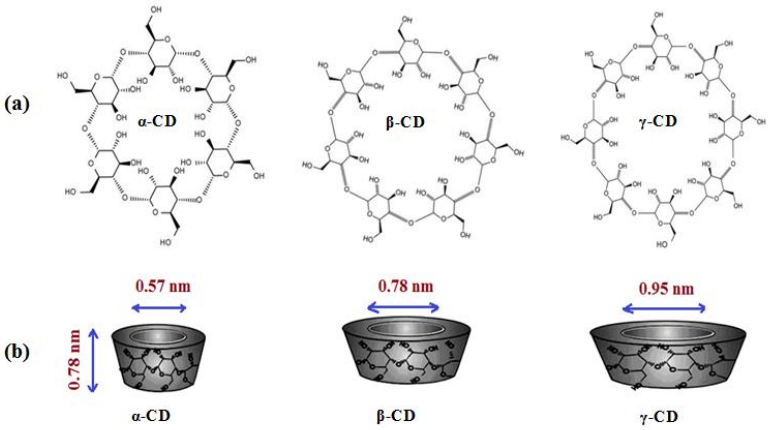

Scheme 2. The structure of L-Tyrosine.

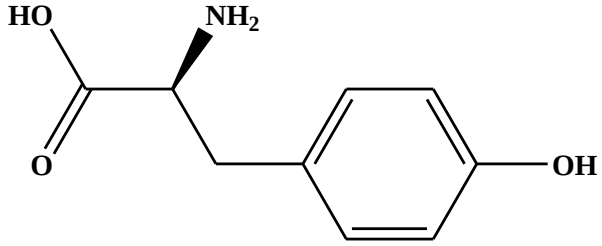

L-TYROSINE

Electrochemical studies of L-Tyrosine at GCE in presence of β-cyclodextrin

The electrochemical studies of L-Tyrosine at GCE in the presence of β-cyclodextrin in 0.1 M H_2SO_4 as supporting electrolyte with 100 mVs^{-1} scan rate in pH~ 7 buffers. The low signal is the cyclic voltammogram of L-TY for bare GCE. The voltammetric response is apparently improved in the presence of $12x10^{-3}$ mM of β-cyclodextrin (Fig.5a and 5b) respectively. It demonstrated that only one oxidation peak can be seen at three electrodes in the potential range from 0 to +1.90 V (Fig. 5a). No reduction peak was observed in the redox process, suggesting that the electrochemical reaction is a totally irreversible process. As can be seen, L-TY oxidation peaks at the bare GCE are all broad due to slow electron transfer, and a poorly defined oxidation peak with very low current was observed at +1.67 V in 100 mVs^{-1} scan rate (Bare GCE). Also, an oxidation peak at +1.77 V with low current was obtained at GCE (L-TY/GCE). However, under identical conditions, the oxidation peak current of L-TY/β-CD at GCE. The peaks were broad and their oxidation peak potentials concurrently shift positively in comparison with that of bare GCE (L-TY/ β-CD/GCE). The highest improvement of the oxidation peak current and the smallest positive shift oxidation peak potential were obtained at the L-TY/β-CD at GCE. For example, a 2.7×10^{-3} M L-TY gave an oxidation peak at +1.77 V with a peak current of +0.9661 μA at GCE and an oxidation peak at +1.79 V with a peak current of +1.1362 μA at L-TY/β-CD/GCE. Both the remarkable peak current enhancement and the positive shift of oxidation peak potential are undoubtedly attributed to the unique characteristics of β-CD.

Scheme 3. Space filling with Wire mesh structure of anionic (SDS), cationic (CTAB) and non-ionic (TRX-100) surfactants

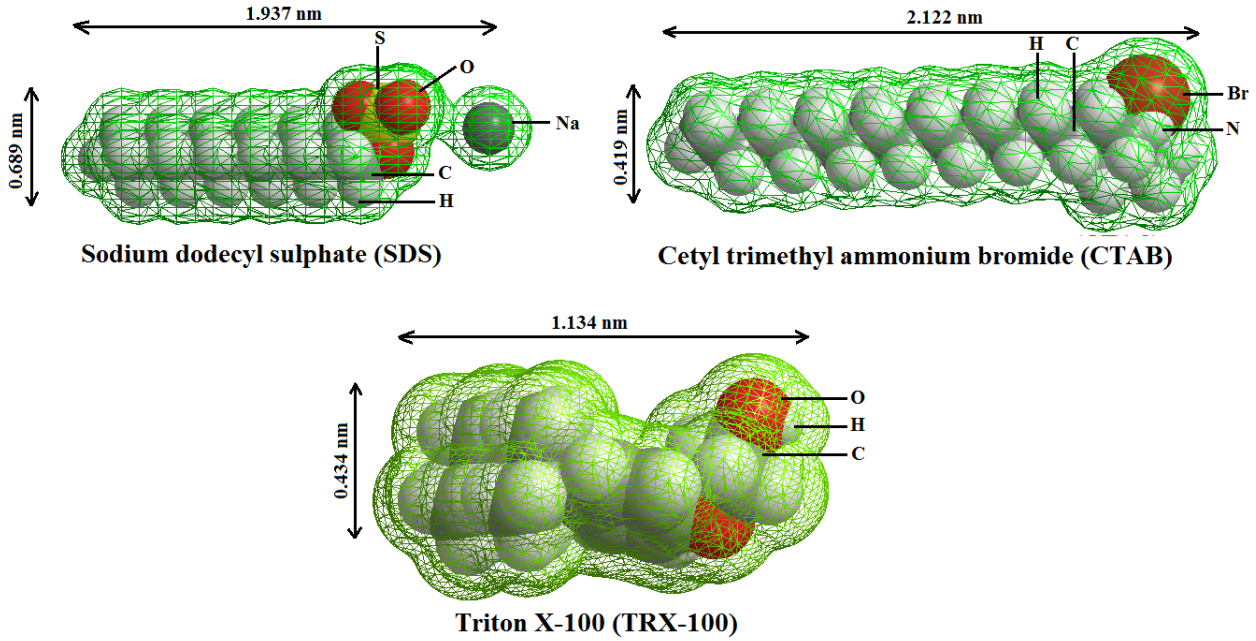

Scheme 4. The possible mechanism of the electrochemical oxidation of L-Tyrosine in acid, neutral and base medium

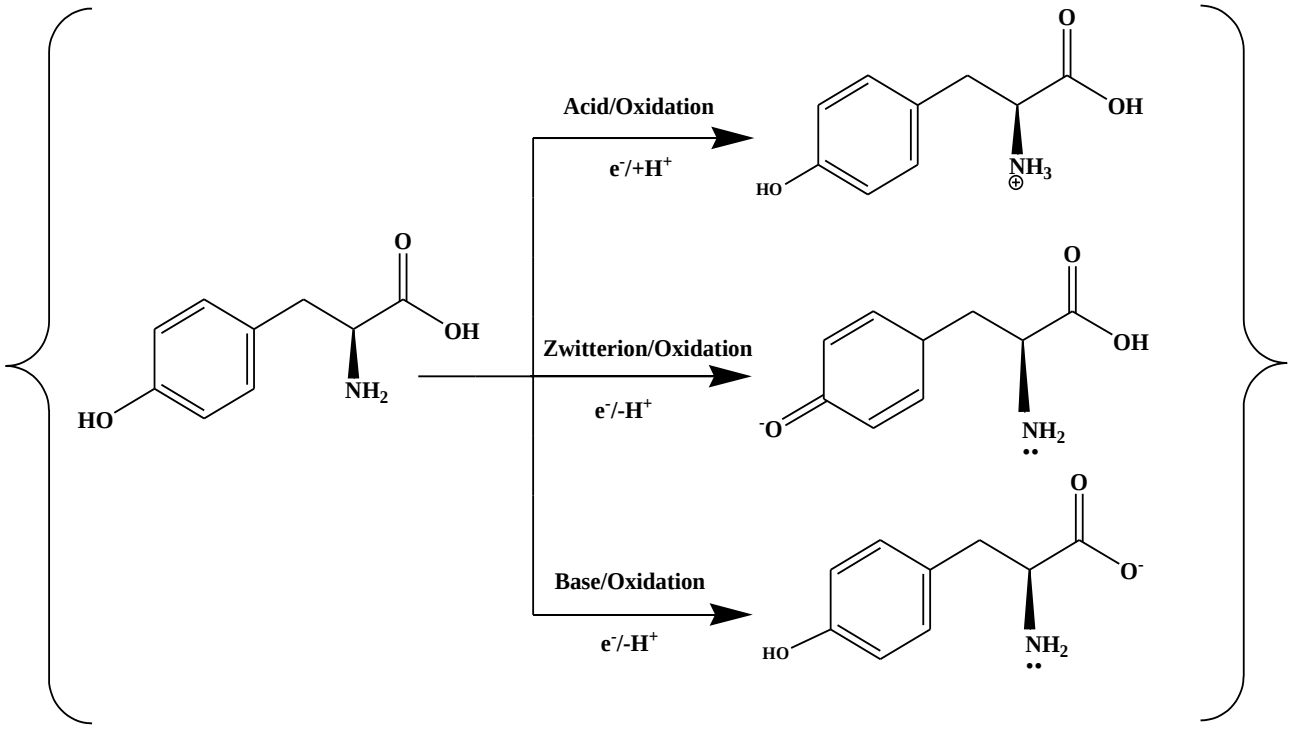

Scheme 5. Schematic diagram of L-Tyrosine with β-Cyclodextrin and surfactants for the interactions

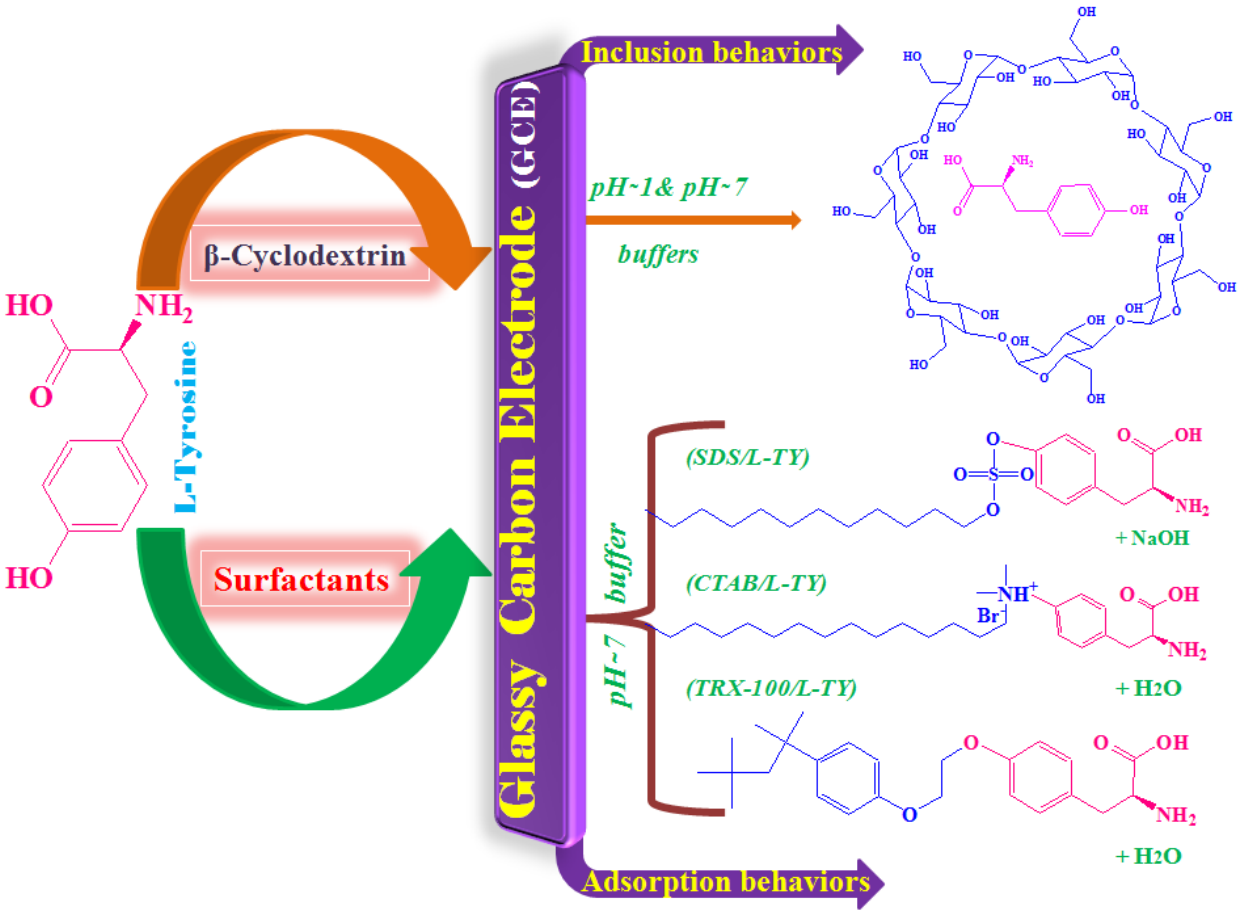

Scheme 6. Space filling with Wire mesh structure of L-Tyrosine and β-Cyclodextrin (L-TY:β-CD) for inclusion complex process.

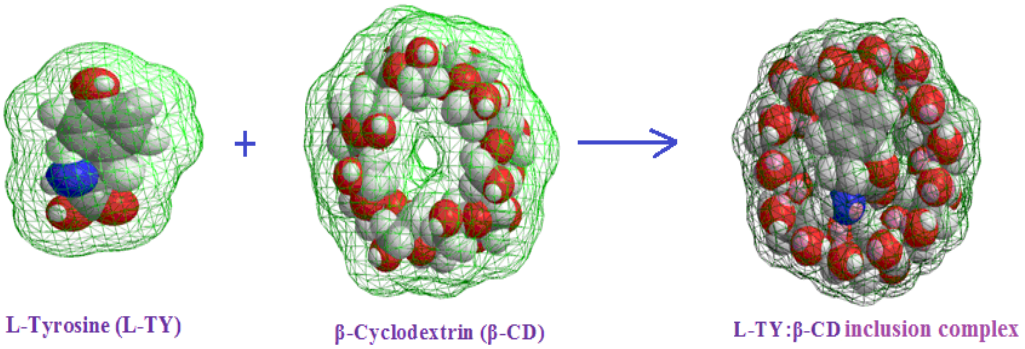

Electrochemical studies of L-Tyrosine at SDS/GCE

To study the effect of addition of surfactant the experiment were carried out using anionic surfactant SDS. Initially, cyclic voltammogram were recorded GCE a solution containing L-TY ($2.7x10^{-3}$ M) in phosphate buffer solution at pH~7. Keeping the concentration of L-TY constant, the concentration of the surfactant was increased from 0 to 5 x 10^{-4} mM. Fig. 6 shows the effect of surfactant concentration both the I_{pa} and I_{pc} decreases rapidly with the increases of surfactant concentration. Its cyclic voltammogram exhibits an anodic (E_{pa} = +0.2313 V and +1.3456 V) and corresponding cathode peaks with (E_{pc} = -0.7161 V) and the difference between the anodic and cathodic peak potential (E_{pa}-E_{pc}/2 = 473

mV and 663 mV) at scan rate of 100 mVs^{-1}. The electrochemical anodic and cathodic peak current goes on decreasing with shifting anodic peak potential (E_{pa}) towards negative and cathodic peak potential (E_{pc}) with negligible shifting from 0 to $5x10^{-4}$ mM. The graph was obtained linearly decreased with respect peak current with increase and I_{pa} proportional to the concentration of SDS. L-TY completely changed gives the anodic peak current (I_{pa}) +0.1043 μA and +0.3362 μA and the cathodic peak current (I_{pc}) -0.1532 μA in $5x10^{-4}$ mM SDS in the pH~7 buffer respectively. From the plot of $1/I-I_0$ versus 1/[SDS] of concentration as shown in Fig.6 (inset figure), the current decreases approximately in linear approach as described by y = 0.0003x + 0.5478; R^2 = 0.9923 and y = 0.0006x + 0.961; R^2 = 0.9941 for the anodic and y = - 0.00062x +13.40; R^2 = 0.9902 for the cathodic peak currents.

Electrochemical studies of L-Tyrosine at CTAB/GCE

To study the effect of addition of surfactant the experiment were carried out using anionic surfactant CTAB. Initially, cyclic voltammogram were recorded GCE a solution containing L-TY ($2.7x10^{-3}$ M) in phosphate buffer solution at pH~7. Keeping the concentration of L-TY constant, the concentration of the surfactant was increased from 0-$5x10^{-4}$ mM. Fig. 7 shows the effect of surfactant concentration both the I_{pa} and I_{pc} increases rapidly with the increases of surfactant concentration. Its cyclic voltammogram exhibits an anodic (E_{pa} = +0.8924 V and +1.2139 V) and corresponding cathode peaks with (E_{pc} = -0.4821 V) and the difference between the anodic and cathodic peak potential (E_{pa}-E_{pc}/2 = 687 mV and 848 mV) at scan rate of 100 mVs^{-1}. The electrochemical anodic and cathodic peak current goes on increasing with shifting anodic peak potential (E_{pa}) towards positive and cathodic peak potential (E_{pc}) with negligible shifting from $5x10^{-4}$ mM – 0 mM. The graph was obtained linearly increased with respect peak current with increase and I_{pa} proportional to the concentration of CTAB. L-TY completely changed gives the anodic peak current (I_{pa}) +4.5753 μA and +3.4359 μA and cathodic peak current (I_{pc}) -1.4126 μA in $5x10^{-4}$ mM CTAB in the pH~7 buffer respectively. From the plot of $1/I-I_0$ versus 1/[CTAB] of concentration as shown in Fig.7 (inset figure), the current increases approximately in linear approach as described by y = 0.0002x + 0.2544; R^2 = 0.9858 and y = 0.0001x + 0.3711; R^2 = 0.9898 for the anodic and y = -0.00001x – 0.8588; R^2 = 0.9823 for the cathodic peak currents.

Electrochemical studies of L-Tyrosine at TRX-100/GCE

To study the effect of addition of surfactant the experiment were carried out using anionic surfactant TRX-100. Initially, cyclic voltammogram were recorded GCE a solution containing L-TY ($2.7x10^{-3}$ M) in phosphate buffer solution at pH~7. Keeping the concentration of L-TY constant, the concentration of the surfactant was increased from 0 - $5x10^{-4}$ mM. Fig. 8 shows the effect of surfactant concentration both the I_{pa} and I_{pc} decreases rapidly with the increases of surfactant concentration. Its cyclic voltammogram exhibits an anodic (E_{pa} = +1.4727 V) and corresponding cathode peaks with (E_{pc} = -0.9187 V) and the difference between the anodic and cathodic peak potential (E_{pa}-E_{pc}/2 = 1195 mV) at scan rate of 100 mVs^{-1}. The electrochemical anodic and cathodic peak current goes on decreasing with shifting anodic peak potential (E_{pa}) towards negative and cathodic peak potential (E_{pc}) with negligible shifting from 0 - $5x10^{-4}$ mM. The graph was obtained linearly decreased with respect peak current with increase and I_{pa} proportional to the concentration of TRX-100. L-TY completely changed gives the anodic peak current (I_{pa}) +1.2622 μA and cathodic peak current (I_{pc}) -0.0292 μA in $5x10^{-4}$ mM TRX-100 in the pH~7 buffer respectively. From the plot of $1/I-I_0$ versus 1/[TRX-100] of concentration as shown in Fig.8 (inset figure), the current decreases approximately in linear approach as described by y= 0.00006x + 0.6692; R^2= 0.9921 for the anodic and y= -0.0003x –0.6692; R^2= 0.9889 for the cathodic peak currents.

Electrochemical studies of L-Tyrosine at GCE in presence of surfactants

The three types of surfactants viz (SDS-anionic), (CTAB-cationic) and (Triton X-100-non ionic) were used for electrochemical studies of L-TY. The electrochemical studies of L-TY at glassy carbon electrode in the presence of trace amount of surfactants onto the surface as well as into the solution were studied in 0.1M H_2SO_4 as supporting electrolyte with 100 mVs^{-1} scan rate. Therefore by preparing the L-TY in pH~7 makes possible the enhancement of both oxidation as well as reduction peaks compared among all surfactants. The voltammetric response is apparently improved in the presence of $5x10^{-4}$ mM of SDS, CTAB and TRX-100 (Fig.9a and 9b) respectively. With the gradual increase in the CTAB concentration as well as both the peak current and peak potential differ. These results also suggest that completeness of surfactants concentration below $5x10^{-4}$ mM.

It demonstrated that only one oxidation peak can be seen at three electrodes in the potential range

from -1.2 to +2.0 V (Fig. 9a). Clearly, one reduction peak was observed in the redox process, suggesting that the electrochemical reaction is a reversible and irreversible process. As can be seen, L-TY oxidation peaks at the bare GCE are all broad due to slow electron transfer, and a poorly defined oxidation peak with very low current was observed at +1.67 V in 100 mVs^{-1} scan rate (Bare GCE). Also, an oxidation peak at +1.77 V with low current was obtained at GCE (L-TY/GCE). However, under identical conditions, the oxidation peak (+1.79 V current of L-TY/TRX-100, +1.4 V current of L-TY/SDS and +0.8 V L-TY/CTAB) and the reduction peak only appear (-0.5 V current of L-TY/CTAB) at GCE. The peaks were highly broad and their oxidation peak potentials concurrently shift negatively in comparison with that of bare GCE, L-TY/TRX-100/GCE and L-TY/SDS/GCE than L-TY/CTAB/GCE. The highest improvement of the oxidation and reduction peak current and the largest negative shift oxidation and reduction peak potential were obtained at the L-TY/CTAB/GCE. For example, a 2.7×10^{-3} M L-TY gave an oxidation peak at +1.77 V with a peak current of 0.9661 μA (no reduction peak) at GCE and an oxidation peak at +0.87 V with a peak current of (+4.5753 μA) and reduction peak –0.48 V with a peak current of (-.4126 μA) at L-TY/CTAB/GCE. Both the remarkable peak current enhancement and the negative shift of oxidation peak potential are undoubtedly attributed to the unique characteristics of surfactants.

Table 1. Cyclic voltammetric study for L-TY:β-CD in pH~1 buffer, scan rate 100 mV s^{-1}, L-TY (Conc.$2.7x10^{-3}$ M) solution in various concentration of β-CD (0–$12x10^{-3}$M).

β-CD (M)	E_{pa} (V)	I_{pa} (μA) x 10^{-5}	E_{pc} (V)	I_{pc} (μA) x 10^{-5}	E_{pa}-E_{pc}/2 (mV)
Without(0.000)	1.0356	0.8792	-0.5801	-0.6794	807
0.002	1.0313	0.9030	-0.5793	-0.6817	805
0.006	1.0227	0.9613	-0.5633	-0.6936	793
0.008	1.0217	0.9680	-0.5601	-0.7089	790
0.010	1.0206	0.9902	-0.5548	-0.7131	787
0.012	1.0174	1.1005	-0.5537	-0.7553	785
Slope		0.0007		-0.0011	
Binding constant (M^{-1})		324		514	
Correlation coefficient (R^2)		0.9070		0.9320	
ΔG (KJ mol^{-1})		-32811.3		-36214.8	

Table 2. Cyclic voltammetric study for L-TY:β-CD in pH~7 buffer, scan rate 100 mV s^{-1}, L-TY (Conc.2.7x10^{-3} M) solution in various concentration of β-CD (0–12x10^{-3}M).

β-CD (M)	E_{pa1} (V)	I_{pa1} (µA) x 10^{-5}	E_{pa2} (V)	I_{pa2} (µA) x 10^{-5}	E_{pc} (V)	I_{pc} (µA) x 10^{-5}	E_{pa}-E_{pc}/2 (mV)	
		1		2			1	2
Without (0.000)	0.1771	1.8301	0.6582	1.6412	-0.4867	-1.4227	332	572
0.0002	0.2847	1.3534	0.6613	1.2124	-0.6527	-1.4727	469	657
0.004	0.3091	1.0629	0.69	1.0202	-0.7382	-1.4004	524	714
0.006	0.3213	0.0925	0.6924	0.099	-0.7577	-1.2689	539	725
0.008	0.3359	0.0839	0.6997	0.0986	-0.7699	-1.1978	552	735
0.010	0.3604	0.0797	0.707	0.0844	-0.7772	-1.1517	569	742
0.012	0.3628	0.0711	0.7168	0.0839	-0.7943	-1.1506	578	755
Slope		0.0045		0.0065		-0.051		
Binding constant (M^{-1})		138		142		69		
Correlation coefficient (R^2)		0.9983		0.9837		0.9935		
ΔG (KJ mol^{-1})		-28585.1		-28717.8		-24563.9		

Table 3. Cyclic voltammetric study for L-TY: SDS in pH~ 7 buffers, scan rate 100 mV s^{-1}, L-TY (Conc.2.7x10^{-3} M) solution in various concentration of SDS (0–5x10^{-4}mM).

SDS (mM)	E_{pa1} (V)	I_{pa1} (µA) x 10^{-4}	E_{pa2} (V)	I_{pa2} (µA) x 10^{-4}	E_{pc} (V)	I_{pc} (µA) x 10^{-4}	E_{pa}-E_{pc}/2 (mV)	
		1		2			1	2
Without (0.000)	0.2903	0.2033	1.3584	0.7604	-0.6143	-0.2055	452	631
0.0001	0.28	0.1724	1.3563	0.6210	-0.6282	-0.2034	454	636
0.0002	0.2604	0.1545	1.3520	0.5084	-0.6752	-0.1937	467	661
0.0003	0.2544	0.1353	1.3514	0.4086	-0.6816	-0.1705	468	661
0.0004	0.2488	0.1203	1.3508	0.3650	-0.6944	-0.1546	471	662
0.0005	0.2313	0.1043	1.3456	0.3362	-0.7161	-0.1532	473	663
Slope		0.0003		0.0006		-0.0062		
Binding constant (M^{-1})		3193		364		154		

Correlation coefficient (R^2)	0.9923	0.9941	0.9902
ΔG (KJ mol^{-1})	-46811.24	-34212.5	-29222.2

Table 4. Cyclic voltammetric study for L-TY: CTAB in pH~ 7 buffers, scan rate 100 mV s^{-1}, L-TY (Conc.2.7x10^{-3} M) solution in various concentration of CTAB (0–5x10^{-4}mM).

CTAB (mM)	E_{pa1} (V)	I_{pa1} (µA) x 10^{-4}	E_{pa2} (V)	I_{pa2} (µA) x 10^{-4}	E_{pc} (V)	I_{pc} (µA) x 10^{-4}	E_{pa}-E_{pc}/2 (mV)	
		1		2			1	2
Without (0.000)	1.1755	1.6585	1.2406	1.7122	-0.7438	-0.4258	960	992
0.0001	0.8679	2.1136	1.2342	2.3715	-0.6573	-0.9835	762	945
0.0002	0.8753	2.9267	1.2278	2.8033	-0.637	-1.1184	756	932
0.0003	0.8818	3.7865	1.2225	3.1335	-0.5131	-1.2918	697	867
0.0004	0.8828	4.2423	1.2171	3.2321	-0.4901	-1.3507	686	854
0.0005	0.8924	4.5753	1.2139	3.4359	-0.4821	-1.4126	687	848
Slope		0.0002		0.0001	-0.00001			
Binding constant (M^{-1})		1092		2185	21857			
Correlation coefficient (R^2)		0.9858		0.9898	0.9823			
ΔG (KJ mol^{-1})		-40586.5		-44610.1	-57970.5			

Table 5. Cyclic voltammetric study for L-TY: TRX-100 in pH~ 7 buffers, scan rate 100 mV s^{-1}, L-TY (Conc.2.7x10^{-3} M) solution in various concentration of TRX-100 (0–5 x 10^{-4}mM).

TRX-100 (mM)	E_{pa} (V)	I_{pa} (µA) x 10^{-4}	E_{pc} (V)	I_{pc} (µA) x 10^{-4}	E_{pa}-E_{pc}/2 (mV)
Without (0.000)	0.9803	2.525	-0.8065	-1.5805	893
0.0001	1.4151	1.7684	-0.7157	-1.2017	1065
0.0002	1.4396	1.3681	-0.8044	-0.0578	1122
0.0003	1.462	1.3604	-0.8364	-0.0527	1149
0.0004	1.4685	1.2637	-0.8781	-0.0379	1173
0.0005	1.4727	1.2622	-0.9187	-0.0292	1195

Slope	0.00006	-0.0003
Binding constant (M^{-1})	15974	31934
Correlation coefficient (R^2)	0.9921	0.9889
ΔG (KJ mol^{-1})	-56147.7	-60170.5

Table 6. Cyclic voltammetric study for L-TY: CTAB, SDS, TRX-100 in pH~ 7 buffers, scan rate 100 mV s^{-1}, L-TY (Conc.2.7x10^{-3} M) solution in various concentration of CTAB, SDS, TRX-100 (0–5x10^{-4}mM).

	Oxidation peak current- I_{pa} (µA) x 10^{-4}			Reduction peak current- I_{pc} (µA) x 10^{-4}		
Surfactants Conc.	**SDS**	**CTAB**	**TRX-100**	**SDS**	**CTAB**	**TRX-100**
0	0.2033	1.6585	2.525	-0.2055	-0.4258	-1.5805
0.1	0.1724	2.1136	1.7684	-0.2034	-0.9835	-1.2017
0.2	0.1545	2.9267	1.3681	-0.1937	-1.1184	-0.0578
0.3	0.1353	3.7865	1.3604	-0.1705	-1.2918	-0.0527
0.4	0.1203	4.2423	1.2637	-0.1546	-1.3507	-0.0379
0.5	0.1043	4.5753	1.276	-0.1532	-1.4126	-0.0292

Effect of various surfactants in the electro-oxidation of L-Tyrosine

Effects of various surfactants for the oxidation of L-TY were investigated. Figs. 6, 7 and 8, clearly shows that the concentration of surfactants exhibits remarkable enhancement effect on the oxidation and reduction peak current of L-TY. However, the oxidation and reduction peak current of L-TY is closely related to the concentration of SDS, CTAB, TRX-100. The oxidation and reduction peak current is increases and decreases as the function of surfactants concentration from 0-5x10^{-4} mM, SDS, CTAB, TRX-100 surfactants the current gradually increased and decreased while increasing the concentration. The graph shows the concentration versus I_{pa} and I_{pc} was obtained very good linearity with correlation coefficient (R^2); SDS = 0.9923, 0.9941 and 0.9902, CTAB = 0.9858, 0.9898 and 0.9823, TRX-100 = 0.9921 and 0.9889 respectively. L-TY changes at oxidation peak current (I_{pa}) is +0.1043 µA and +0.3362 µA , +4.5753 and +3.4359 µA, +1.2622 µA and reduction peak current (I_{pc}) is -0.1532 µA, -1.4126 µA, -0.0292 µA in various SDS, CTAB, TRX-100 concentrations in pH~7 buffer respectively.

The peak current of L-TY changes at oxidation and reduction reaction in various SDS (Fig.10a), CTAB (Fig.10b) and TRX-100 (Fig.10c) concentrations in pH~7 buffer respectively. Comparative cyclic voltammograms of 5x10^{-4} mM SDS, CTAB and TRX-100 are also shown in the Fig.11a and 11b.

Among these surfactants, the CTAB was showed excellent electrochemical activity for the investigation of L-TY. The trace amount of CTAB (i.e. 5x10^{-4} mM) was enhanced both anodic and cathodic peak current signals on the GCE. The CTAB could increase the polarity on the surface of glassy carbon electrode, which response in the enhancement of current signals. The concentration of CTAB was varied from 0 to 5x10^{-4} mM. The current response for among the surfactants, CTAB surfactant was more

electro catalytic behavior compared than SDS and TRX-100.

4. Conclusion

The following conclusion can be arrived at from the above studies; (i) the host-guest inclusion complexes of L-Tyrosine (L-TY) with β-Cyclodextrin (β-CD) were confirmed by electrochemical study using Benesi-Hildebrand plot. (ii) The electrochemical study of L-TY with surfactants (SDS, CTAB and TRX-100) for the adsorption behaviors indicates good electro catalytic activity towards the oxidation of L-TY in presence of surfactants. CTAB adsorbs on the GCE surface individually with its hydrophobic C-H chains close to the surface, thereby increasing the surface area and its positive charged head groups directs towards the bulk solution. In acidic media L-TY exists in anionic form and interacts with positive charged head groups of CTAB through electrostatic interactions. However, the anionic surfactants such as SDS and non-ionic surfactants such as TRX-100 will improve the oxidation/reduction peak current. CTAB was shows excellent enhancement in both oxidation and reduction peak currents than SDS and TRX-100.

Acknowledgment

One of the author, S.Mohandoss wishes to thank UGC for providing the financial assistance in the scheme of RFSMS-BSR to carry out this work.

References

Alan, T et al., **(2003).** "Polymers Processed with Cyclodextrin Inclusion Compounds" National Textile Center Research Briefs – Materials Competency: M02-NS01.

Carlsson, A et al., **(1978).** "Dependence of 5-HT and catecholamine synthesis on concentrations of precursor amino-acids in rat brain" Naunyn-Schmiedeberg's Archives of Pharmacology. 303: 157-164.

Carmen, Q et al., **(2010).** "Nanostructures on gold electrodes for the development of an L-Tyrosine electrochemical sensor based on host–guest supramolecular interactions" Sensors and Actuators B. 149: 129–135.

Chung, J et al., **(2006).** "α-Cyclodextrin-modified infrared chemical sensor for selective determination of tyrosine in biological fluids" Analytical Biochemistry. 359: 124–131.

Fang, W et al., **(2006).** "Spectrofluorimetric Determination of the Substrates Based on the Fluorescence Formation with the Peroxidase-Like Conjugates of Hemie with Proteins" Analytical Letters. 25: 1469-1478.

Geoffrey, N et al., **(1987).** "Electrochemistry of Biphenyl derivatives of cobalt in solutions of anionic and cationic micelles" J. Electroanal. Chem. 233: 173-187.

Gharibi, H et al., **(2000).** "Electrochemical studies of interaction between ceyltrimethylammonium bromide and α-, β-cyclodextrins at various temperatures" Colloids and Surfaces A: Physicochemical and Engineering Aspects. 175: 361–369.

Hu, S et al., **(1991).** "Determination of progesterone based on the enhancement effect of surfactants in linear sweep polarography" Analytica Chimica Acta. 248: 103-108.

Huei, C et al., **(2008).** "Development of an aminocarboxylic acid-modified infrared chemical sensor for selective determination of tyrosine in urine" Analytica Chimica Acta. 606: 230–238.

James, F et al., **(1991).** "Controlling electrochemical catalysis with surfactant microstructures" Acc. Chem. Res. 24 (3): 75–81.

Kagan, K et al., **(2009).** "Electrochemical detection of protein tyrosine kinase-catalysed phosphorylation using gold nanoparticles" Biosensors and Bioelectronics. 24: 1484–1489.

Kenneth, A et al., **(2009).** "Electropolymerized tyrosine-based thin films: Selective cell binding via peptide recognition to novel electropolymerized biomimetic tyrosine RGDY films" Analytical Biochemistry. 384: 86–95.

Li, C et al., **(2006).** "Voltammetric determination of tyrosine based on an L-serine polymer film electrode" Colloids and Surfaces B: Biointerfaces. 50: 147–151.

Longzhen, Z et al., **(2008).** "Synthesis of a novel β -cyclodextrin derivative with high solubility and the electrochemical properties of ferrocene-carbonyl-β-cyclodextrin inclusion complex as an electron transfer mediator" Electrochemistry Communications. 10: 340–345.

MacDonald, S. M. et al., **(1996).** "Electrochemical oxidation reactions of tyrosine, tryptophan and related dipeptides" Electrochimica Acta. 42: 1189-1200.

Ming, C et al., **(2006).** "Study of inclusion complex of β-cyclodextrin and nitrobenzene" Chemosphere.63: 522–529.

Nada, F et al., **(2007).** "Effect of surfactants on the voltammetric response and determination of an antihypertensive drug" Talanta. 72: 1438–1445.

Pappenheimer, J. R. et al., **(1936).** "The Surface Tension of Aqueous Solutions of Dipolar Ions" Journal of American Chemical Society.58 (10):1851–1855.

Qiao, X et al., **(2005).** "Electrocatalytic Oxidation and Direct Determination of L-Tyrosine by Square Wave Voltammetry at Multi-wall Carbon Nanotubes Modified Glassy Carbon Electrodes" Microchimica Acta. 151: 47-52.

Sabine, L et al., **(1997).** "Determination of the L-DOPA/ L-tyrosine ratio in human plasma by high-performance liquid chromatography Usefulness as a marker in metastatic malignant melanoma" Journal of Chromatography B. 696: 9–17.

Sanfeliu, M.C et al., **(2003).** "Determination of tyrosine through a FIA-direct chemiluminescence procedure" Talanta. 60: 369-376.

Shanmugam, M et al., **(2008).** "Host–guest interaction of L-Tyrosine with β-cyclodextrin" Spectrochimica Acta Part A. 71: 125–132.

Srinivasan, K et al., **(2012).** "Spectral and electrochemical study of host–guest inclusion complex between 2,4-dinitrophenol and β-cyclodextrin" Spectrochimica Acta Part A. 94: 89–100.

Srinivasan, K et al., **(2011).** "Study of inclusion complex of β-cyclodextrin and diphenylamine: Photophysical and electrochemical behaviors" Spectrochimica Acta Part A. 79: 169–178.

Srinivasan, K et al., **(2011).** "Study of inclusion complex of β-cyclodextrin and Ortho-Anisidine; photophysical and electrochemical behaviors" Journal of Molecular Structure. 987: 214–224.

Szejtli, J et al., **(1982).** "Cyclodextrins and their inclusion complexes" Journal of Chromatography. 253: 138.

Xintao, S et al., **(2001).** "Formation of and Coalescence from the Inclusion Complex of a Biodegradable Block Copolymer and α-Cyclodextrin: A Novel Means To Modify the Phase Structure of Biodegradable Block Copolymers" Macromolecules. 34 (21): 7355–7361.

Yi, H et al., **(2001).** "Adsorption stripping voltammetry of phenol at Nafion-modified glassy carbon electrode in the presence of Surfactants" Talanta. 55: 1205–1210.

Ying, H et al., **(2006).** "Separation and determination of L-Tyrosine and its metabolites by capillary zone electrophoresis with a wall-jet amperometric detection" Talanta. 70: 1157–1163.

****